

Theoretical analysis of screw dislocations and image forces in anisotropic multilayered media

Chien-Ching Ma* and Hsin-Tai Lu

Department of Mechanical Engineering, National Taiwan University, Taipei, Taiwan 10617, Republic of China

(Received 15 November 2005; published 5 April 2006)

The elastic field induced by a screw dislocation embedded in an anisotropic elastic multilayered medium is presented in this study. A linear coordinate transformation is introduced in this study to simplify the problem. The explicit complete solutions of shear stresses and displacement for this problem consist only of the simplest solutions for a screw dislocation in an infinite homogeneous medium. The physical meaning of the solution is the image method and the magnitudes and locations of image screw dislocations are determined automatically from the mathematical method presented in this study. With the aid of the Peach-Koehler equation, the explicit forms of image forces exerted on screw dislocations are easily derived from the full-field solutions of stresses. Numerical results for full-field stress distributions in multilayered media subjected to a screw dislocation are presented. The image forces and equilibrium positions of a screw dislocation, two screw dislocations, and an array of screw dislocations are presented by numerical calculations and are discussed in detail.

DOI: [10.1103/PhysRevB.73.144102](https://doi.org/10.1103/PhysRevB.73.144102)

PACS number(s): 61.72.Lk, 68.35.Dv

I. INTRODUCTION

The layered half-plane subjected to surface traction is of very wide applicability in a number of engineering fields. For example, the coating of a thin layer to protect soft matrices under contact and friction is a particular case of the problem. Furthermore, a wide range of electronic components are now manufactured by depositing semiconducting layers on supporting substrates. Because of the rapid expansion in the use of structural components made of laminated materials, predictions of the behavior of multilayered media subjected to arbitrary loads or dislocations are needed. In multilayered structure, each layer is bonded to either substrate or another layer already bonded to the substrate. Dislocations can degrade the physical properties in semiconductor devices where the multilayered structures are commonly used. There exists the misfit dislocation which accommodates the lattice mismatch between the two layers. The prediction of the critical film thickness to get dislocation-free films has been an important subject of many investigations. Dislocation-free crystalline films grown epitaxially on substrates of different crystals are of considerable interest due to their important applications in the semiconductor and electro-optical device industry. The film and substrate generally have different crystal lattice parameters and the lattice mismatch produces internal stress in the system. This internal stress is the driving force for the formation of misfit dislocation. The dislocation-free film is energetically unfavorable above a critical thickness and misfit dislocations are introduced spontaneously into the epitaxial interface, which cause the degradation of the device performance. Modeling of dislocation behavior in thin films promises provide a better insight into device design using epitaxy technology. Also important is the investigation of the movement of the dislocation, which in turn entails the determination of force on a dislocation due to the interface and the free surface. In order to understand the motion of a dislocation in an elastic material, one needs to calculate the stress distribution induced by the dislocation. The materials having multilayered structures such as the thin film on films or substrate used in semi-

conductor devices are usually anisotropic, therefore, it is believed that the analysis for the anisotropic multilayered medium is required. Solutions for the elasticity field induced by a dislocation are useful to provide a direct means of determining the Peach-Koehler (or image) force, which is of direct relevance in understanding the characteristics of the behavior of real dislocations.

Anti-plane shear deformations are the two-dimensional problem that has many applications in anisotropic or isotropic elastic bodies. For the anti-plane shear deformation, the displacement is parallel to the axial coordinate that is normal to the plane and is dependent only on the coordinates in the plane. Such deformation field characterized by a single axial displacement can be regarded as complementary to that of plane strain deformation. The anti-plane problem plays a useful role as a pilot problem that reveals simpler aspects of elasticity solutions. Anisotropic elasticity has been an active research subject for recent years due to its applications to composite materials. Ting¹ provided many basic discussions and investigated some fundamental problems for anisotropic anti-plane deformations. Analysis of anisotropic elasticity problems is often tedious due to the presence of many elastic constants. It is desirable to reduce the dependence on elastic constants through theoretical considerations in advance of the analysis of a given boundary value problem. For anisotropic elasticity, Lekhnitskii's formulation² and Stroh's formulation³ are the two widely used methods. The general solutions obtained by these methods showed that the anti-plane anisotropic problem can be converted to a corresponding isotropic problem by properly changing the geometry of the original configuration and the tractions on the boundary. In other words, the anisotropic anti-plane problem can be simplified to an isotropic problem with the aid of a suitable coordinate transformation. The properties of the coordinate transformations for anti-plane deformations have been investigated by Ma⁴ and Horgan and Miller.⁵ An orthotropic transformation concept was introduced by Yang and Ma⁶ to analyze the very complicated and difficult in-plane deformations for planar anisotropic solids.

For homogeneous elastic material in an unbounded medium, the elastic field around dislocations or concentrated loadings is generally well known. Many research ventures start by addressing problems in a semi-infinite plane subjected to concentrated forces or dislocations, the simplest example of medium with boundary, for the first step of analysis. Heed⁷ solved the problem for the isotropic half-plane. Ting and Barnett⁸ discussed the relation between the image force on dislocation and the half-plane with fixed boundary for anisotropic material. Further work on the bimaterial which is perfectly bonded of two semi-infinite materials, had been done by Dundurs and Sendekyj⁹ for isotropic material and Barnett and Lothe,¹⁰ Suo,¹¹ and Ting¹² for the anisotropic case. Barnett and Lothe¹³ studied the Peach-Koehler image force for a straight dislocation parallel to the interface of two perfectly bonded dissimilar elastic half-spaces. They proved that for proportional anisotropic biomaterial, the dislocation is repelled from the interface when it is located in the elastically softer half-space and is attracted to the interface when it is located in the stiffer half-space. The advance and more complicated problem is supplied by a loading in an infinite strip or in an infinite layer bonded on a semi-infinite substrate. Nabano and Kostlan¹⁴ and Moss and Hoover¹⁵ solved the problem of an edge dislocation in an isotropic strip with free surfaces simultaneously. A similar problem of an orthotropic strip was completed by Chou.¹⁶ Stagni and Lizzio¹⁷ obtained the elastic field of an isotropic infinite strip by means of the complex variable method. Wu and Chiu¹⁸ and Chiu and Wu¹⁹ obtained the solution of an anisotropic infinite strip subjected to dislocations and concentrated forces from eigenfunction expansion by residue theory, respectively. The stress distribution of an edge dislocation in an isotropic layered half-plane was investigated by Weeks *et al.*²⁰ and Lee and Dundurs.²¹ Chu²² investigated the problem of a screw dislocation lying in two perfectly bonded layers, each of which is isotropic with the same finite thickness.

The use of the image method in solving two-dimensional isotropic problems dealing with screw dislocations is well known and has been used successfully for simple cases. It was found that an infinite number of image screw dislocations were required for finite configurations. The concepts of semi-reflection and semi-transmission mirrors were used to determine the magnitudes and locations of the image screw dislocations without solving the boundary value problem.^{23–25} The multiple image problem for screw dislocations then becomes combinatorial problem of counting reflections and transmissions for a given image path length. Basically, one can extend this methodology to include any number of layers, but as the number of layers increases, obtaining an explicit solution becomes extremely laborious and time consuming. Hence the work was not extended beyond the five-layer case (with three finite lengths) by Kamat *et al.*²⁴ and Öveçoğlu *et al.*²⁵ It is impossible to use the conventional image method to obtain the solution of anisotropic multilayered problem directly. Thus, the Green's function method to solve the elasticity problem is more general and applicable to various geometries, although the mathematics involved may become tedious. However, the existing methods are difficult to apply directly to solve complicated problems.

The most complicated problem of the interaction between a screw dislocation and an anisotropic multilayered medium, which is the object of the present paper, has not been previously confronted. The material properties and the thickness in each layer are different. By using the Fourier transform technique and a series expansion, an effective analytical methodology developed by Lin and Ma²⁶ is used in this study to construct explicit analytical solutions for an anisotropic multilayered medium with n layers due to a screw dislocation in an arbitrary layer. A general linear coordinate transformation is introduced in this study to simplify the problem. This linear coordinate transformation will simplify the governing equilibrium equation without complicating the boundary and interface continuity conditions. Based on this transformation, the original anisotropic multilayered problem is converted to an equivalent isotropic multilayered problem. The analytical solutions for the stresses and displacement obtained in this study are exact and are expressed in an explicit closed form. The complete solutions consist only of the simplest solutions for an infinite homogeneous medium with a screw dislocation. It can be shown that the physical meaning of the solution obtained in this study is the image method. The magnitudes and locations of image singularities will be determined automatically from the mathematic method presented in the study. Based on the full-field solutions of stresses and the Peach-Koehler equation, the explicit expressions of image forces exerted on screw dislocations (one dislocation, two dislocations, and an array of dislocations) are easily derived and can be used for numerical calculation with extreme accuracy. For numerical examples, a multilayered medium with ten layers for isotropic materials and eight layers for anisotropic material are discussed in detail. We focus our attention mainly on the numerical calculation of image forces for a screw dislocation, two screw dislocations and an array of screw dislocations. The number of equilibrium point, the equilibrium position and the stability of screw dislocations embedded in the anisotropic multilayered medium are investigated and interesting phenomena of image forces are presented.

II. BASIC EQUATIONS AND LINEAR COORDINATE TRANSFORMATION

Anisotropic material having a symmetric plane at $z=0$ is considered in this study, in which the in-plane and anti-plane deformations are uncoupled. For two-dimensional problems, the Cartesian coordinate system is chosen such that the anti-plane deformation is in the z direction. Let u , v , and w , respectively, represent the displacement components in the x , y , and z directions of the Cartesian coordinate system. For anti-plane shear deformations,

$$u = v = 0, \quad w = w(x, y), \quad (1)$$

the relevant shear stresses are denoted by τ_{yz} and τ_{xz} . The shear stresses are related to the displacement as follows

$$\tau_{yz} = C_{45} \frac{\partial w}{\partial x} + C_{44} \frac{\partial w}{\partial y}, \quad (2)$$

$$\tau_{xz} = C_{55} \frac{\partial w}{\partial x} + C_{45} \frac{\partial w}{\partial y}. \quad (3)$$

In the absence of body forces, the equilibrium equation in the Cartesian coordinate can be written in terms of the displacement w as

$$C_{55} \frac{\partial^2 w}{\partial x^2} + 2C_{45} \frac{\partial^2 w}{\partial x \partial y} + C_{44} \frac{\partial^2 w}{\partial y^2} = 0. \quad (4)$$

Equation (4) is the governing equation for an anisotropic anti-plane deformation problem and is a homogeneous second-order partial differential equation for displacement w . Such a linear partial differential equation can be transformed into the Laplace equation by a linear coordinate transformation.^{4,5} A special linear coordinate transformation is introduced as

$$\begin{bmatrix} X \\ Y \end{bmatrix} = \begin{bmatrix} 1 & \alpha \\ 0 & \beta \end{bmatrix} \begin{bmatrix} x \\ y \end{bmatrix}, \quad (5)$$

where $\alpha = -\frac{C_{45}}{C_{44}}$, $\beta = \frac{\mu}{C_{44}}$, and $\mu = \sqrt{C_{44}C_{55} - C_{45}^2}$. Assume that C_{44} and C_{55} as well as $\sqrt{C_{44}C_{55} - C_{45}^2}$ are all positive. μ can be considered as the effective material constant for the anisotropic solid. After the coordinate transformation, Eq. (4) can be rewritten as the standard Laplace equation in the (X, Y) coordinate system

$$\mu \left(\frac{\partial^2 w}{\partial X^2} + \frac{\partial^2 w}{\partial Y^2} \right) = 0. \quad (6)$$

It is interesting to note that the mixed derivative disappears from Eq. (4) and Eq. (6) has the same form as the equilibrium equation for the isotropic material in the (X, Y) coordinate. The relationships between the displacement and shear stresses in the two coordinate systems (x, y) and (X, Y) are given by

$$w(x, y) = w(X, Y), \quad (7)$$

$$\tau_{yz}(x, y) = \mu \frac{\partial w(X, Y)}{\partial Y} = \tau_{YZ}(X, Y), \quad (8)$$

$$\begin{aligned} \tau_{xz}(x, y) &= \beta \mu \frac{\partial w(X, Y)}{\partial X} - \alpha \mu \frac{\partial w(X, Y)}{\partial Y} \\ &= \beta \tau_{XZ}(X, Y) - \alpha \tau_{YZ}(X, Y). \end{aligned} \quad (9)$$

We can see that the expression of $w(X, Y)$ and $\tau_{YZ}(X, Y)$ in Eqs. (7) and (8) in the (X, Y) coordinate have the same forms as that in the isotropic material with the effective shear modulus μ . Hence for the boundary value problems, such as the anisotropic multilayered medium considered, only the displacement w and the shear stress τ_{yz} are involved in the boundary and continuity conditions. In a mathematical sense, Eqs. (1)–(4) are transformed to Eqs. (6)–(9) by the linear coordinate transformation expressed in Eq. (5), or in a physical sense, the governing equation (4) and the stress displacement relations (2) and (3) of an anisotropic anti-plane problem are converted into an equivalent isotropic problem by properly changing the geometry of the body using the linear

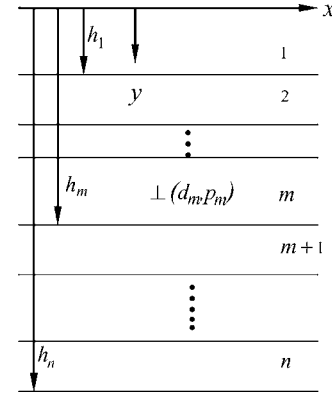


FIG. 1. Configuration and x - y coordinates system of an anisotropic multilayered medium.

coordinate transformation, Eq. (5). The coordinate transformation in Eq. (5) has the following characteristics: (a) it is linear and continuous, (b) an anisotropic problem is converted to an isotropic problem after the transformation, and (c) there is no stretching and rotation in the horizontal direction. These important features offer advantages in dealing with straight boundaries and interfaces in the multilayered system discussed in the present study. The most interesting feature is that a straight line $(x_1, y_0), (x_2, y_0)$ that is parallel to the x axis will remain a straight line $(X_1, Y_0), (X_2, Y_0)$ parallel to the X axis after the transformation, and the length of the line will not change, i.e., $X_2 - X_1 = x_2 - x_1$.

III. FULL-FIELD SOLUTIONS FOR A SCREW DISLOCATION IN AN ANISOTROPIC MULTILAYERED MEDIUM

In this section, the Green's function for an anisotropic n -layered medium with a screw dislocation located in an arbitrary layer will be constructed. Consider an anisotropic multilayered medium with n layers subjected to a screw dislocation of magnitude b_z along the z -axis located in the m th layer as shown in Fig. 1. Here n and m are arbitrary integers. The location of this screw dislocation is (d_m, p_m) . The displacement equilibrium equation in each layer is expressed as

$$C_{55}^j \frac{\partial^2 w^j}{\partial x^2} + 2C_{44}^j \frac{\partial^2 w^j}{\partial x \partial y} + C_{44}^j \frac{\partial^2 w^j}{\partial y^2} = 0, \quad j = 1, 2, \dots, n. \quad (10)$$

The traction-free boundary conditions on the top and bottom surfaces of the multilayered medium are

$$\tau_{yz}^1(x, 0) = 0, \quad \tau_{yz}^n(x, h_n) = 0. \quad (11)$$

The jump condition for the displacement at the m th layer is

$$w^{m+}(x, p_m^+) - w^{m-}(x, p_m^-) = b_z H(x - d_m), \quad (12)$$

where $H(\cdot)$ is the Heaviside function. In Eq. (12), w^{m+} and w^{m-} indicate the displacement above and below the plane of the applied screw dislocation in the m th layer; p_m^+ and p_m^- denote the positions just above and below the applied screw

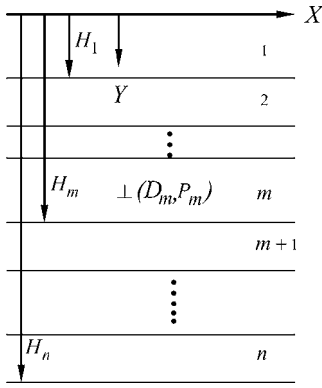


FIG. 2. Configuration and X - Y coordinates system for the multilayered medium after the linear coordinate transformation.

dislocation at $y=p_m$ (see Fig. 1). Application of the traction and displacement continuity conditions at the interface between the j th and $j+1$ -th layer yields

$$\begin{aligned} \tau_{yz}^j(x, h_j) &= \tau_{yz}^{j+1}(x, h_j), \\ w^j(x, h_j) &= w^{j+1}(x, h_j). \end{aligned} \quad j = 1, 2, \dots, n-1. \quad (13)$$

The linear coordinate transformation described by Eq. (5) can be used to solve the anisotropic anti-plane problem for only a single material constant in each layer. However, for a multilayered anisotropic medium with straight interfaces shown in Fig. 1, a new linear coordinate transformation which is a modification of Eq. (5) will be used to transform the multilayered anisotropic problem to an equivalent multilayered isotropic problem. In order to maintain the geometry of the layered configuration, the linear coordinate transformation described in Eq. (5) is modified for each layer as follows,

$$\begin{bmatrix} X \\ Y \end{bmatrix} = \begin{bmatrix} 1 & \alpha_j \\ 0 & \beta_j \end{bmatrix} \begin{bmatrix} x \\ y \end{bmatrix} + \sum_{k=1}^{j-1} h_k \begin{bmatrix} \alpha_k - \alpha_{k+1} \\ \beta_k - \beta_{k+1} \end{bmatrix}, \quad j = 1, 2, \dots, n, \quad (14)$$

where $\alpha_j = -\frac{C_{45}^j}{C_{44}^j}$, $\beta_j = \frac{\mu_j}{C_{44}^j}$, and $\mu_j = \sqrt{C_{44}^j C_{55}^j - (C_{45}^j)^2}$. Comparing with Eq. (5), the first term in the right-hand side of Eq. (14) retains exactly the same form while the second summation term becomes the modified term. The geometric configuration in the transformed (X, Y) coordinate is shown in Fig. 2. Note that while the thickness of each layer is changed, the interfaces are still parallel to the X axis. Thus, the new geometric configuration is similar to the original problem.

The equilibrium equations in the transformed coordinate are governed by the standard Laplace equation expressed by

$$\mu_j \left(\frac{\partial^2 w^j}{\partial X^2} + \frac{\partial^2 w^j}{\partial Y^2} \right) = 0. \quad (15)$$

The displacement w and the shear stress τ_{YZ} are continuous along the interfaces in the transformed coordinates,

$$w^j(X, H_j) = w^{j+1}(X, H_j), \quad \tau_{YZ}^j(X, H_j) = \tau_{YZ}^{j+1}(X, H_j),$$

$$j = 1, 2, \dots, n-1, \quad (16)$$

where

$$H_j = \beta_j h_j + \sum_{k=1}^{j-1} (\beta_k - \beta_{k+1}) h_k.$$

The top and bottom surfaces are traction free and can be expressed as

$$\tau_{YZ}^1(X, 0) = 0, \quad \tau_{YZ}^n(X, H_n) = 0. \quad (17)$$

The jump of the displacement within the m th layer caused by the screw dislocation is

$$w^{m+}(X, P_m^+) - w^{m-}(X, P_m^-) = b_z H(X - D_m), \quad (18)$$

where

$$\begin{aligned} D_m &= d_m + \alpha_m p_m + \sum_{k=1}^{m-1} (\alpha_k - \alpha_{k+1}) h_k, \\ P_m &= \beta_m p_m + \sum_{k=1}^{m-1} (\beta_k - \beta_{k+1}) h_k. \end{aligned} \quad (19)$$

Here w^{m+} and w^{m-} indicate the displacement above and below the screw dislocation in the m th layer. The location of the screw dislocation is shifted from d_m to D_m and from p_m to P_m in the horizontal and vertical directions, respectively, as indicated in Fig. 2. The stress displacement relations expressed in the (X, Y) coordinates for each layer become

$$\begin{aligned} \tau_{XZ}^j(X, Y) &= \mu_j \frac{\partial w^j(X, Y)}{\partial X}, \\ \tau_{YZ}^j(X, Y) &= \mu_j \frac{\partial w^j(X, Y)}{\partial Y}. \end{aligned} \quad (20)$$

The boundary value problem indicated in Eqs. (15)–(20) is similar to the multilayered problem for an isotropic material. Hence the linear coordinate transformation presented in Eq. (14) changes the original anisotropic multilayered problem to the corresponding isotropic multilayered problem with a similar geometric configuration and boundary conditions. The boundary value problem indicated previously can be solved by the integral transform technique. The expressions for the field variables will be found by applying a Fourier transform over the spatial coordinate X and the full field solutions of displacement and shear stresses are explicitly expressed in the (X, Y) coordinate as²⁶

$$w^j(X, Y; D_m, P_m) = \sum_{l=0}^{\infty} \sum_{k=1}^N \frac{M_k}{\pi} \left[b_z \left(-\tan^{-1} \frac{Y - P_m + F_k^{c'}}{X - D_m} + \tan^{-1} \frac{Y + P_m + F_k^{c''}}{X - D_m} + \tan^{-1} \frac{Y + P_m + F_k^{d'}}{X - D_m} - \tan^{-1} \frac{Y - P_m - F_k^{d''}}{X - D_m} \right) \right], \quad (21)$$

$$\tau_{YZ}^j(X, Y; D_m, P_m) = \sum_{l=0}^{\infty} \sum_{k=1}^N \frac{\mu_j M_k}{\pi} \left[b_z \left(\frac{-(X - D_m)}{(X - D_m)^2 + (Y - P_m + F_k^{c'})^2} + \frac{(X - D_m)}{(X - D_m)^2 + (Y + P_m + F_k^{c''})^2} + \frac{(X - D_m)}{(X - D_m)^2 + (Y + P_m - F_k^{d'})^2} - \frac{(X - D_m)}{(X - D_m)^2 + (Y - P_m - F_k^{d''})^2} \right) \right], \quad (22)$$

$$\tau_{XZ}^j(X, Y; D_m, P_m) = \sum_{l=0}^{\infty} \sum_{k=1}^N \frac{\mu_j M_k}{\pi} \left[b_z \left(\frac{Y - P_m + F_k^{c'}}{(X - D_m)^2 + (Y - P_m + F_k^{c'})^2} - \frac{Y + P_m + F_k^{c''}}{(X - D_m)^2 + (Y + P_m + F_k^{c''})^2} - \frac{Y + P_m - F_k^{d'}}{(X - D_m)^2 + (Y + P_m - F_k^{d'})^2} + \frac{Y - P_m - F_k^{d''}}{(X - D_m)^2 + (Y - P_m - F_k^{d''})^2} \right) \right], \quad (23)$$

where

$$\begin{cases} N = 2^{n+j-m-1} \cdot (2^n - 1)^l, & 1 \leq j \leq m, \\ N = 2^{n+m-j-1} \cdot (2^n - 1)^l, & m \leq j \leq n. \end{cases}$$

Here n is the number of layers, m denotes the layer that is subjected to the applied screw dislocation, and j is the j -th layer where the solution is required. The terms M_k , $F_k^{c'}$, $F_k^{c''}$, $F_k^{d'}$, and $F_k^{d''}$ in Eqs. (21)–(23) are very complicated and are explicitly presented in Appendix A. The structures of the complete solutions given in Eqs. (21)–(23) have some interesting characteristics. The solutions are composed of infinite terms, and it is interesting to note that each term represents the solution for a screw dislocation (image screw dislocation) in an infinite homogeneous medium. The locations of image screw dislocations are located at $X=D_m$, $Y=P_m-F_k^{c'}$ (or $Y=-P_m-F_k^{c''}$, $Y=-P_m+F_k^{d'}$, $Y=P_m+F_k^{d''}$). However, M_k represents the magnitude of the image screw dislocation. The locations of image screw dislocations depend on the locations of the interfaces, i.e., H_j , and the magnitude of the image screw dislocation M_k depends only on the reflection and refraction coefficients, i.e., t_j , s_j' , and s_j'' in each layer.

Only one term (the first term) in the infinite series of Eqs. (21)–(23) represents the dislocation b_z in an infinite medium at $X=D_m$ and $Y=P_m$; all the remaining terms are image screw dislocations that are induced to satisfy the boundary and interface conditions. The mathematical derivation in this study provides an automatic determination for the locations and magnitudes of all the image dislocations. Hence, the physical meaning of the solutions presented in Eqs. (21)–(23) is referred to as the method of images. The advantage of this mathematical method used in this study is that the solutions of problems with complicated geometric configurations can be constructed by superposing the solution in an infinite medium. The solutions presented in Eqs.

(21)–(23) are useful to construct formulations of image forces exerted on dislocations in the next section.

Equations (21)–(23) are the solutions in the (X, Y) coordinate system for the problem indicated in Fig. 2. The relationships between the displacement and shear stresses in the two coordinate systems (x, y) and (X, Y) are given in Eqs. (7)–(9). Finally, by substituting X and Y defined in Eq. (14) and the relations of D_m and P_m with d_m and p_m in Eq. (19) into Eqs. (21)–(23), and using the displacement and stress relations in Eqs. (7)–(9), the complete solutions for the original problem of the anisotropic multilayered medium as indicated in Fig. 1 can be obtained from Eqs. (21)–(23) as follows:

$$w^j(x, y; d_m, p_m) = w^j(X, Y; D_m, P_m), \quad (24)$$

$$\tau_{yz}^j(x, y; d_m, p_m) = \tau_{YZ}^j(X, Y; D_m, P_m), \quad (25)$$

$$\tau_{xz}^j(x, y; d_m, p_m) = \beta_j \tau_{XZ}^j(X, Y; D_m, P_m) - \alpha_j \tau_{YZ}^j(X, Y; D_m, P_m). \quad (26)$$

Equations (24)–(26) are the explicit expression of the Green's function for the anisotropic multilayered medium subjected to a screw dislocation located in the m th layer at the position (d_m, p_m) . The solutions for two or more screw dislocations in the anisotropic multilayered medium can be constructed by superposition of the Green's function.

IV. IMAGE FORCES EXERTED ON SCREW DISLOCATIONS IN AN ANISOTROPIC MULTILAYERED MEDIUM

The full-field solutions of a screw dislocation embedded in an anisotropic multilayered medium have already been

analyzed in detail in previous sections. The image forces exerted on screw dislocations will be investigated in this section, which may play an important role in thin film technology in the sense that the movement of the dislocation due to the interaction with the interfaces and the free surfaces can cause the failure of the electronic circuit on the layer. According to the Peach-Koehler formula, the image force exerted on the screw dislocation can be obtained from the stress field at the location of the dislocation minus the self-stresses of the dislocation in an infinite homogeneous material of the m th layer. In Cartesian coordinates, the relations between image forces and stress fields are

$$\begin{bmatrix} F_x^m \\ F_y^m \end{bmatrix} = \begin{bmatrix} -\hat{\tau}_{yz}^m \\ \hat{\tau}_{xz}^m \end{bmatrix} b_z, \quad (27)$$

where F_x^m and F_y^m denote the image force exerted on a screw dislocation at the m th layer along the horizontal and vertical directions, respectively, and $\hat{\tau}_{yz}^m = \tau_{yz}^m - \tau_{yz}^s$, $\hat{\tau}_{xz}^m = \tau_{xz}^m - \tau_{xz}^s$ in which τ_{yz}^m and τ_{xz}^m are the shear stresses in the m th layer given in Eqs. (25) and (26), respectively, τ_{yz}^s and τ_{xz}^s are the self-stresses of the screw dislocation. The self-stresses of a screw dislocation of the Burgers vector b_z in an infinite homogeneous anisotropic medium, which is also presented in the first term in Eqs. (25) and (26), can be written as

$$\tau_{yz}^s = \frac{\mu_m b_z}{2\pi} \frac{-(x-d_m) + \alpha_m(y-p_m)}{[(x-d_m) + \alpha_m(y-p_m)]^2 + \beta_m^2(y-p_m)^2}, \quad (28)$$

$$\tau_{xz}^s = \frac{\mu_m b_z}{2\pi} \left(\beta_m \frac{\beta_m(y-p_m)}{[(x-d_m) + \alpha_m(y-p_m)]^2 + \beta_m^2(y-p_m)^2} + \alpha_m \frac{[(x-d_m) + \alpha_m(y-p_m)]}{[(x-d_m) + \alpha_m(y-p_m)]^2 + \beta_m^2(y-p_m)^2} \right). \quad (29)$$

The force on the dislocation is defined as the negative gradient of the interaction energy. Since the interaction energy does not change if the dislocation were to move parallel to the interface between the layers, it is clear that the force on the dislocation is perpendicular to the interface. The image forces exerted on a screw dislocation located at (d_m, p_m) of the m th layer are easily derived from Eqs. (25) and (29) and the explicit results are

$$F_x^m(d_m, p_m) = 0, \quad (30)$$

$$F_y^m(d_m, p_m) = \frac{b_z^2}{\pi} \mu_m \beta_m \left[\sum_{l=0}^{\infty} \sum_{k=1}^{N^*} M_k^* \left(\frac{1}{F_k^{C'}} - \frac{1}{2P_m + F_k^{C''}} - \frac{1}{2P_m - F_k^{D'}} - \frac{1}{F_k^{D''}} \right) - \frac{1}{f_1^{C'}} \right], \quad m = 1, 2, \dots, n, \quad (31)$$

where $N^* = 2^{n-1}(2^n - 1)^l$, and $P_m = \beta_m p_m + \sum_{k=1}^{m-1} (\beta_k - \beta_{k+1}) h_k$. Since the stresses to be evaluated and the screw dislocation are both located in the m th layer, the terms M_k , $F_k^{C'}$, $F_k^{C''}$, $F_k^{D'}$, and $F_k^{D''}$ in Eqs. (22) and (23) can be simplified to M_k^* , $F_k^{C'}$, $F_k^{C''}$, $F_k^{D'}$, and $F_k^{D''}$, respectively, as indicated in Eq. (31). The terms M_k^* , $F_k^{C'}$, $F_k^{C''}$, $F_k^{D'}$, and $F_k^{D''}$ are explicitly represented in Appendix B. It is important to note that the first term in the summation formulation for $l=0$ and $k=1$ is a singular term which can be exactly cancelled by $\frac{1}{f_1^{C'}}$ (i.e., the self-stress). Hence the result presented in Eq. (31) has no singularity so that the numerical calculation of the image force can be easily and accurately evaluated.

The image forces for problems of multiple dislocations can be obtained by the superposition method. Consider the case that two screw dislocations A and B with the same Burger's vector b_z are located in different (or same) layer. Dislocation A is located in the m th layer at the position (d_m, p_m) and dislocation B is located in the j th layer at the position (d_j, p_j) . The total image force exerted on dislocation A is the summation of Eq. (31) and the image force exerted on dislocation A by dislocation B , which is the shear stresses induced at the position (d_m, p_m) by dislocation B at (d_j, p_j) . The results are

$$F_x^A(d_m, p_m) = F_x^m(d_m, p_m) - b_z \tau_{yz}^m(d_m, p_m; d_j, p_j) = -b_z \tau_{yz}^m(D_m, P_m; D_j, P_j), \quad (32)$$

$$F_y^A(d_m, p_m) = F_y^m(d_m, p_m) + b_z \tau_{xz}^m(d_m, p_m; d_j, p_j) = \frac{b_z^2}{\pi} \mu_m \beta_m \left[\sum_{l=0}^{\infty} \sum_{k=1}^{N^*} M_k^* \left(\frac{1}{F_k^{C'}} - \frac{1}{2P_m + F_k^{C''}} - \frac{1}{2P_m - F_k^{D'}} - \frac{1}{F_k^{D''}} \right) - \frac{1}{f_1^{C'}} \right] + b_z \beta_m \tau_{xz}^m(D_m, P_m; D_j, P_j) - b_z \alpha_m \tau_{yz}^m(D_m, P_m; D_j, P_j), \quad m = 1, 2, 3, \dots, n. \quad (33)$$

The image force exerted on a screw dislocation of an array of infinite screw dislocations with uniform spacing a has important engineering applications and can be constructed by the superposition of available solutions presented previously. Suppose that the array of infinite screw dislocations is located in the m th layer. The image force exerted on any screw dislocation is the same and can be represented as the summation of Eq. (31) and the image force induced by other infinite numbers of screw dislocations. The results can be explicitly represented as follows.

$$F_x^m(d_m, p_m; a) = 0, \quad (34)$$

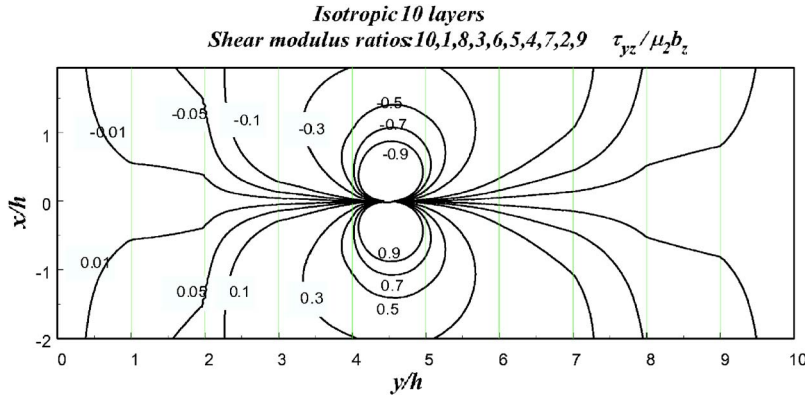


FIG. 3. (Color online) Full-field distribution of the shear stress τ_{yz} for a screw dislocation embedded in the center of the fifth layer for a ten-layered isotropic medium.

$$F_y^m(d_m, P_m; a) = \frac{b_z^2}{\pi} \mu_m \beta_m \left\{ \left[\sum_{l=0}^{\infty} \sum_{k=1}^{N^*} M_k^* \left(\frac{1}{F_k^{C'}} - \frac{1}{2P_m + F_k^{C''}} - \frac{1}{2P_m - F_k^{D'}} - \frac{1}{F_k^{D''}} \right) \right] - \frac{1}{f_1^{C'}} + \sum_{n=1}^{\infty} \sum_{l=0}^{\infty} \sum_{k=1}^{N^*} 2M_k^* \left(\frac{F_k^{C'}}{(na)^2 + (F_k^{C'})^2} - \frac{2P + F_k^{C''}}{(na)^2 + (2P + F_k^{C''})^2} - \frac{2P - F_k^{D'}}{(na)^2 + (2P - F_k^{D'})^2} - \frac{F_k^{D''}}{(na)^2 + (F_k^{D''})^2} \right) \right\}. \quad (35)$$

The explicit results for the image forces as indicated in Eqs. (30)–(35) can be easily written as a FORTRAN program and the image forces can be accurately computed.

V. NUMERICAL RESULTS AND DISCUSSIONS

Computational programs for numerical calculations of the full-field distribution of shear stresses and image forces are constructed by using the explicit expression of the solutions presented in previous sections. The full-field shear stress τ_{yz} for an isotropic multilayered medium consisting of ten layers with constant thickness subjected to a screw dislocation at the center of the fifth layer is shown in Fig. 3. The ratio of the shear modulus, which ranges from 1 to 10, is also indicated in Fig. 3. We can see that τ_{yz} is continuous at the interfaces and approaches zero at the top and bottom boundaries. The image force exerted on a screw dislocation in the ten-layered isotropic medium is indicated in Fig. 4. Except for the sixth layer, in each layer there exists as an equilibrium point, and the locations of these equilibrium points are indicated in Fig. 4. We have four stable equilibrium points and five unstable equilibrium points. It is clearly shown in Fig. 4 that if a layer is softer than two adjacent layers (i.e., the second, fourth, seventh, and ninth layers), then it has a stable equilibrium point. If a layer is stiffer than two adjacent layers (i.e., the first, third, fifth, eighth, and tenth layers), then it has an unstable equilibrium point. However, if a layer is embedded between softer and stiffer layers (i.e., the sixth layer), then it has no equilibrium point.

The material constants and thickness of an anisotropic multilayered medium consisting of eight layers are indicated in Fig. 5. The effective modulus μ for each layer is also shown in Fig. 5, and the larger value of μ means the stiffer of the anisotropic material. The full-field shear stress τ_{yz} for

this anisotropic multilayered medium subjected to a screw dislocation at the center of the fourth layer is shown in Fig. 6. The inclination of the contour for the shear stress in Fig. 6 is due to the anisotropy of the material. The image force exerted on a screw dislocation in the eight-layered anisotropic medium is indicated in Fig. 7. Except for the sixth layer, in each layer there exists as an equilibrium point, and the locations of these equilibrium points are indicated in Fig. 7. We have three stable equilibrium points and four unstable equilibrium points. Similar to the result for isotropic material, if a layer is softer (i.e., the effective shear modulus μ is smaller) than two adjacent layers (i.e., the second, fourth, and seventh layers), then it has a stable equilibrium point.

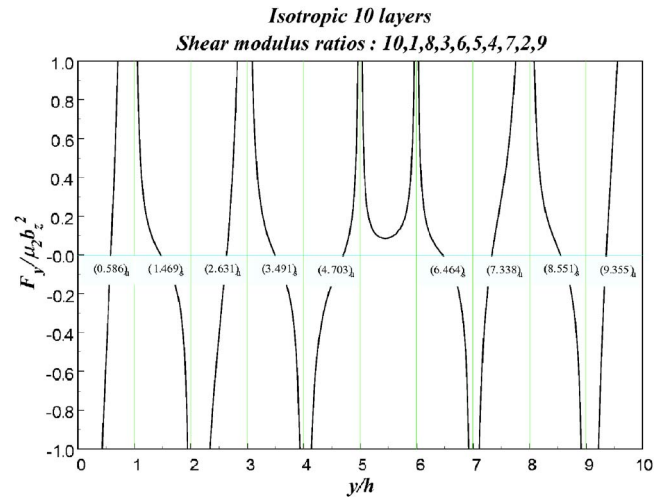


FIG. 4. (Color online) Distribution of the image force, the location and the stability of the equilibrium point for a screw dislocation along the y -axis for the ten-layered isotropic medium.

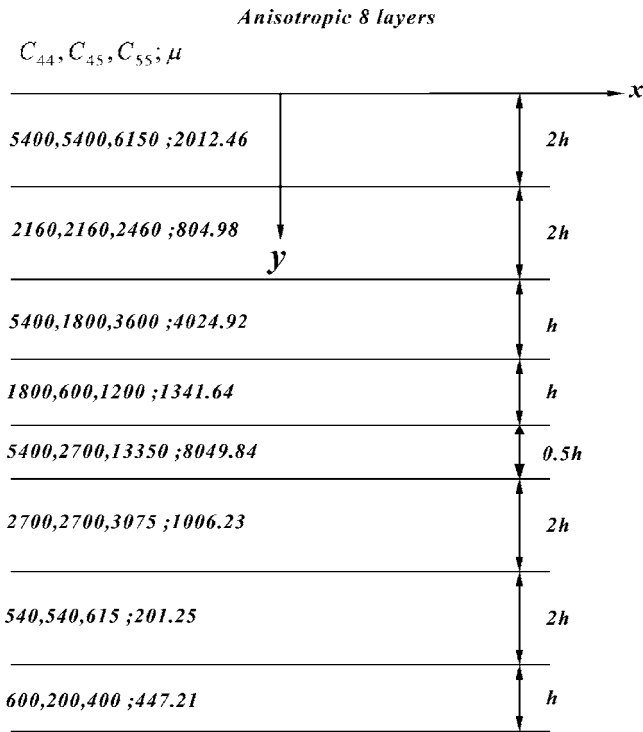


FIG. 5. The material constants and the thickness of each layer for an eight-layered anisotropic medium.

There is no equilibrium point for the sixth layer because the fifth layer is stiffer and the seventh layer is softer than the sixth layer.

Now consider the case that one screw dislocation is located along the y axis, i.e., $(0, y)$, the other screw dislocation is parallel to the first one and is located either on the right-hand side at the position $(0.3h_4, y)$ or on the left-hand side at the position $(-0.3h_4, y)$. The image force exerted on the screw dislocation at $(0, y)$ due to the right (or left) screw dislocation only is shown in Fig. 8 which is just the shear stress τ_{xz} induced by the right (or left) screw dislocation at position $(0, y)$ and is discontinuous at the interfaces. The total image force exerted on the screw dislocation $(0, y)$ is indicated in Fig. 9, which is the summation of the image forces indicated in Figs. 7 and 8. If we compare Fig. 9 with Fig. 7, we can see that the equilibrium points in Fig. 9 are closer to the interfaces than that in Fig. 7 and it has quite different phenomenon for the other screw dislocation located on the right or left side of the screw dislocation. There is no

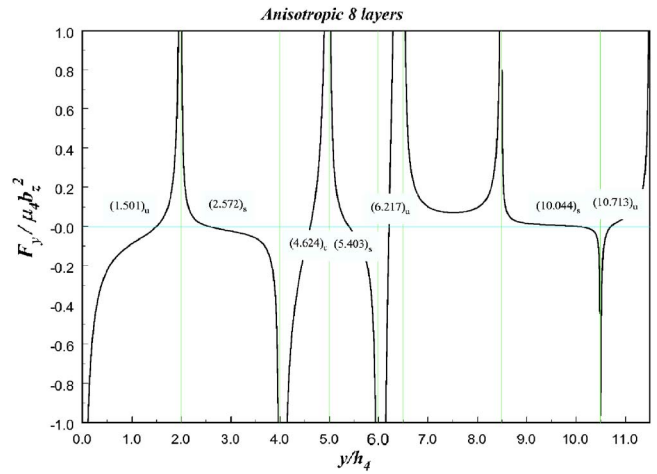


FIG. 7. (Color online) Distribution of the image force, the location, and the stability of the equilibrium point for a screw dislocation along y -axis for an eight-layered anisotropic medium.

equilibrium point for the sixth layer as indicated in Fig. 7, however, we have two equilibrium points, one is stable and the other one is unstable for the sixth layer if the other screw dislocation is located on the right-hand side.

Next, the case of two screw dislocations A and B with the same sign is considered; screw dislocation B is located at the fourth layer and at the position $(0.3h_4, 5.5h_4)$, screw dislocation A is moving along the y axis. The image force exerted on screw dislocation A by screw dislocation B only is shown in Fig. 10 and the discontinuity at the interfaces is observed. Since the screw dislocation B is located in the fourth layer, the image force exerted on the screw dislocation A as shown in Fig. 10 changes sign at this layer. The screw dislocation B has only little contribution on the image force for screw dislocation A except it locates in the adjacent two layers (i.e., the third and fifth layers) and the same layer (i.e., the fourth layer). The total image force exerted on screw dislocation A is indicated in Fig. 11, which is the summation of the image forces in Fig. 7 and Fig. 10. We can see that the screw dislocation B has a significant influence on the image force of the screw dislocation A when these two screw dislocations are located in the same layer, i.e., the fourth layer. It is interesting to note that the number of equilibrium points at the fourth layer changes from one in Fig. 7 to three in Fig. 11, i.e., one unstable and two stable equilibrium points. It is concluded from Figs. 9 and 11 that the equilibrium position

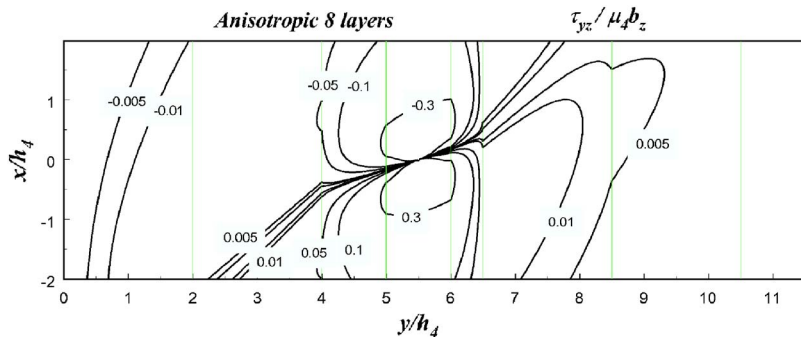


FIG. 6. (Color online) Full-field distribution of the shear stress τ_{yz} for a screw dislocation embedded in the center of the fourth layer for an eight-layered anisotropic medium.

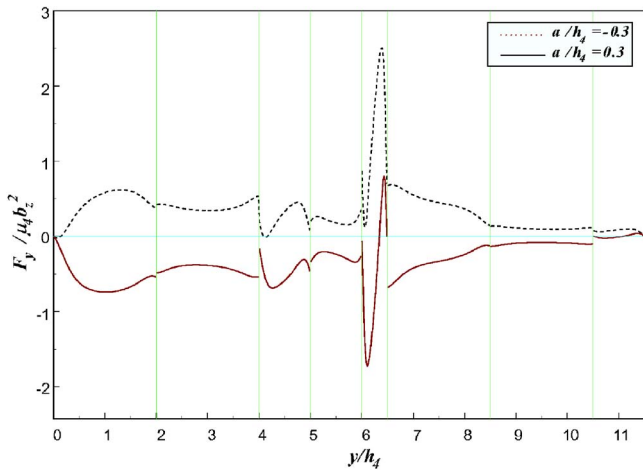


FIG. 8. (Color online) Distribution of the image force for a screw dislocation along y -axis due to the other screw dislocation located at the right (or left) hand side of the screw dislocation.

and the number of equilibrium points of a screw dislocation are significantly influenced by the other screw dislocation located in the same layer.

Finally, an infinite array of dislocations with a uniform spacing a in an anisotropic multilayered medium as indicated in Fig. 5 is considered. The image force exerted on a screw dislocation by the other infinite number of screw dislocation only is shown in Fig. 12 for different spacing ($a = 0.1, 0.2, 0.3h_4$). Obviously, the contribution of the image force from the other infinite number of screw dislocations is larger if the spacing a is smaller. The total image force exerted on the screw dislocation is indicated in Fig. 13, which is clearly shown in Fig. 13 that the equilibrium points are moved toward the interface. Hence it can be concluded that an array of dislocations is most likely to stack near the interface.

VI. CONCLUDING REMARKS

The present paper provides explicit solutions of the stress field and image forces for screw dislocations embedded in an

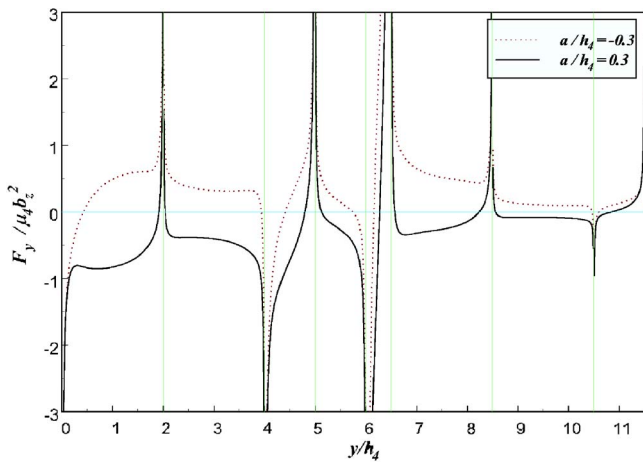


FIG. 9. (Color online) Distribution of the total image force for two screw dislocations, i.e., the summation of Figs. 7 and 8.

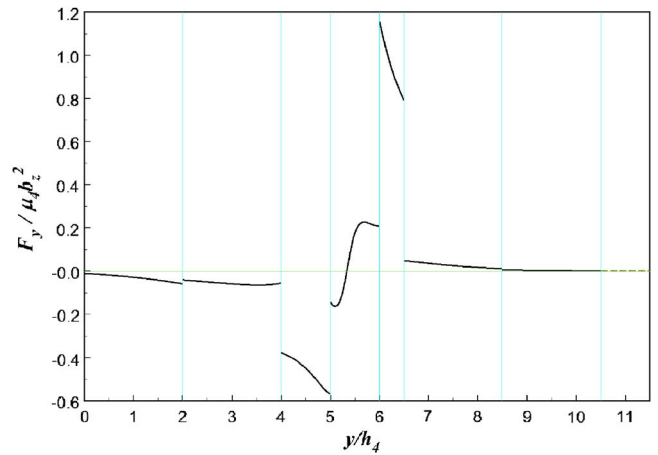


FIG. 10. (Color online) The image force exerted on screw dislocation A by screw dislocation B only, which is located at the fourth layer and at the position $(0.3h_4, 5.5h_4)$.

anisotropic multilayered medium. A general linear coordinate transformation for multilayered media was introduced to simplify the problem without complicating the boundary and interface continuity conditions. With this linear coordinate transformation, the original anisotropic multilayered problem can be reduced to an equivalent isotropic multilayered problem. By using the Fourier transform technique and a series expansion, analytical solutions for displacement and stresses are presented in an explicit form. The complete solutions for this complicated problem consist only of very simple solutions obtained from an infinite homogeneous medium with screw dislocations. Except for the original applied loading, the remaining terms in the infinite series are image screw dislocations which are induced to satisfy the boundary and interface conditions. The mathematical approach used in this study provides an automatic determination for the locations and magnitudes of all the image screw dislocations induced by the interfaces and boundaries. Computational programs for numerical calculations of the full-field shear stresses and image forces exerted on screw dislocations are easily constructed by using the explicit formulation of the solutions.

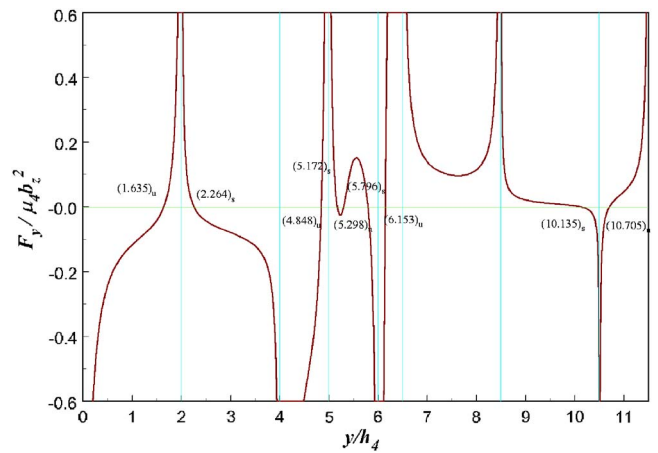


FIG. 11. (Color online) Distribution of the total image force for screw dislocation A, i.e., the summation of Figs. 7 and 10.

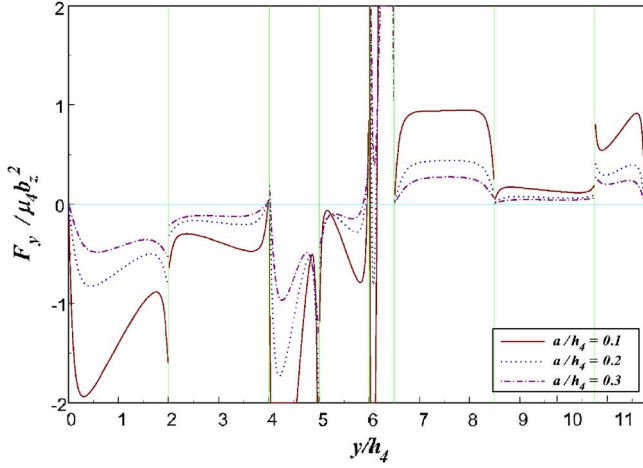


FIG. 12. (Color online) The image force exerted on a screw dislocation by the other infinite number of screw dislocations only for different spacing ($a=0.1, 0.2, 0.3h_4$).

The image forces and equilibrium positions of a screw dislocation, two screw dislocations, and an array of screw dislocations are presented by numerical calculations and are discussed in detail. It is found that the stability of the equilibrium point for a screw dislocation in an anisotropic multilayered medium mainly depends on the effective shear modulus of the two adjacent layers. Generally speaking, if a layer is softer (stiffer) than the two adjacent layers, then there is a stable (unstable) equilibrium point. However, if a layer is embedded between softer and stiffer adjacent layers, then there is no equilibrium point. The image force, the lo-

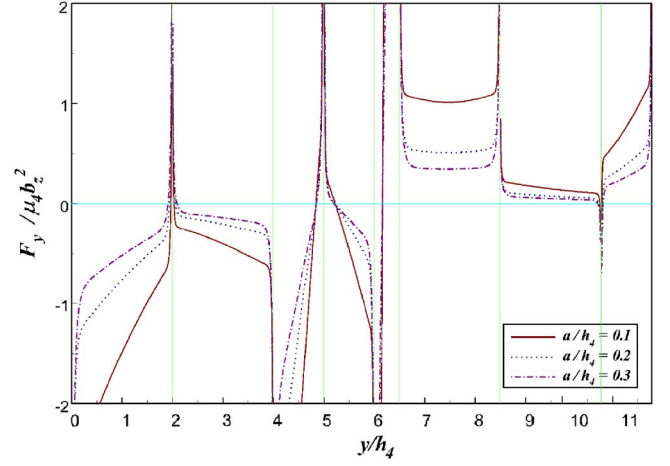


FIG. 13. (Color online) Distribution of the total image force for an array of dislocations for different spacing ($a=0.1, 0.2, 0.3h_4$), i.e., the summation of Figs. 7 and 12.

cation, and the stability of the equilibrium point of a screw dislocation are strongly influenced by other screw dislocations in the same layer. Furthermore, the position of equilibrium points of an array of screw dislocations is located very near the interface.

ACKNOWLEDGMENTS

The financial support of the authors from the National Science Council, Republic of China, through Grant No. NSC 90-2212-E002-230 to National Taiwan University is gratefully acknowledged.

APPENDIX A

The following functions are first defined as

$$\begin{cases} a_1 = 1, f_1^A = 0, \\ a_{i+2^{k-1}} = a_i t_k, & k = 1, 2, \dots, m-1, \\ f_{i+2^{k-1}}^A = -(f_i^A + 2H_k), & i = 1, 2, \dots, 2^{k-1}. \end{cases} \quad (\text{A1})$$

where $t_k = \frac{\mu_{k+1} - \mu_k}{\mu_k + \mu_{k+1}}$ is the reflection coefficient,

$$\begin{cases} b_1 = 1, f_1^{B1} = -2H_n, f_1^{B2} = 0, \\ b_{i+2^{k-1}} = -b_i t_{n-k}, & k = 1, 2, \dots, n-m, \\ f_{i+2^{k-1}}^{B1} = -(f_i^{B1} + 2H_n + 2H_{n-k}), & i = 1, 2, \dots, 2^{k-1}, \\ f_{i+2^{k-1}}^{B2} = -(f_i^{B2} + 2H_n - 2H_{n-k}). \end{cases} \quad (\text{A2})$$

$$\begin{cases} r_{(i-1) \cdot 2^{n-m+k}}^p = -a_i b_k, & r_{2^{n-1} + (k-1) \cdot 2^{m-1} + i}^p = a_i b_k, & i = 1, 2, \dots, 2^{m-1}, \\ g_{(i-1) \cdot 2^{n-m+k}}^p = f_i^A + f_k^{B2}, & g_{2^{n-1} + (k-1) \cdot 2^{m-1} + i}^p = f_k^{B1} - f_i^A, & k = 1, 2, \dots, 2^{n-m}. \end{cases} \quad (\text{A3})$$

$$\begin{cases} r_k^{(l)} = \prod_{o=1}^l r_{i_o}^p, & i_1, i_2, i_3, \dots, i_l = 2, 3, \dots, 2^n, \\ g_k^{(l)} = \sum_{o=1}^l g_{i_o}^p, & k = \sum_{o=1}^{l-1} (i_o - 2)(2^n - 1) + (i_l - 1), \end{cases} \quad (\text{A4})$$

for $l=0$, $r_{i_0}^{(0)}=1$, and $g_{i_0}^{(0)}=0$.

For the case of $1 \leq j \leq m$, the following functions are defined:

$$\begin{cases} f_{(i-1) \cdot 2^{n-m+k}}^{c'} = f_k^{B_2} + f_i^A, \\ f_{(i-1) \cdot 2^{n-m+k}}^{c''} = f_k^{B_1} + f_i^A, & i = 1, 2, \dots, 2^{j-1}, \\ f_{(i-1) \cdot 2^{n-m+k}}^{d'} = f_k^{B_2} - f_i^A, & k = 1, 2, \dots, 2^{n-m}, \\ f_{(i-1) \cdot 2^{n-m+k}}^{d''} = f_k^{B_1} - f_i^A. \end{cases} \quad (\text{A5})$$

Finally, the terms M_k , $F_k^{c'}$, $F_k^{c''}$, $F_k^{d'}$ and $F_k^{d''}$ indicated in Eqs. (21)–(23) can be expressed explicitly as

$$\begin{cases} M_{(k-1) \cdot 2^{n+j-m-1+i}} = \frac{-1}{2} \left(\prod_{o=j}^{m-1} s_o' \right) r_k^{(l)} r_l^p, \\ F_{(k-1) \cdot 2^{n+j-m-1+i}}^{c'} = g_k^{(l)} + f_i^{c'}, & k = 1, 2, \dots, (2^n - 1)^l, \\ F_{(k-1) \cdot 2^{n+j-m-1+i}}^{c''} = g_k^{(l)} + f_i^{c''}, & i = 1, 2, \dots, 2^{n+j-m-1}, \\ F_{(k-1) \cdot 2^{n+j-m-1+i}}^{d'} = g_k^{(l)} + f_i^{d'}, \\ F_{(k-1) \cdot 2^{n+j-m-1+i}}^{d''} = g_k^{(l)} + f_i^{d''}, \end{cases} \quad (\text{A6})$$

where $s_o' = \frac{2\mu_{o+1}}{\mu_o + \mu_{o+1}}$ is the refraction coefficient.

For the case of $m \leq j \leq n$, the expressions are

$$\begin{cases} f_{(i-1) \cdot 2^{m-1+k}}^{c'} = f_i^{B_1} - f_k^A, \\ f_{(i-1) \cdot 2^{m-1+k}}^{c''} = f_i^{B_1} + f_k^A, & i = 1, 2, \dots, 2^{n-j}, \\ f_{(i-1) \cdot 2^{m-1+k}}^{d'} = f_i^{B_2} - f_k^A, & k = 1, 2, \dots, 2^{m-1}, \\ f_{(i-1) \cdot 2^{m-1+k}}^{d''} = f_i^{B_2} + f_k^A. \end{cases} \quad (\text{A7})$$

The terms M_k , $F_k^{c'}$, $F_k^{c''}$, $F_k^{d'}$, and $F_k^{d''}$ are presented by

$$\begin{cases} M_{(k-1) \cdot 2^{n-j+m-1+i}} = \frac{1}{2} \left(\prod_{o=m}^{j-1} s_o'' \right) r_k^{(l)} r_{2^{n-1+i}}^p, \\ F_{(k-1) \cdot 2^{n-j+m-1+i}}^{c'} = g_k^{(l)} + f_i^{c'}, & k = 1, 2, \dots, (2^n - 1)^l, \\ F_{(k-1) \cdot 2^{n-j+m-1+i}}^{c''} = g_k^{(l)} + f_i^{c''}, & i = 1, 2, \dots, 2^{n+m-j-1}, \\ F_{(k-1) \cdot 2^{n-j+m-1+i}}^{d'} = g_k^{(l)} + f_i^{d'}, \\ F_{(k-1) \cdot 2^{n-j+m-1+i}}^{d''} = g_k^{(l)} + f_i^{d''}, \end{cases} \quad (\text{A8})$$

where $s_o'' = \frac{2\mu_o}{\mu_o + \mu_{o+1}}$ is the refraction coefficient.

APPENDIX B

The terms M_k^* , $F_k^{C'}$, $F_k^{C''}$, $F_k^{D'}$, and $F_k^{D''}$ indicated in Eq. (31) are expressed as follows:

$$M_{(k-1) \cdot 2^{n-1+i}}^* = \frac{-1}{2} r_k^{(l)} r_i^p, \quad k = 1, 2, \dots, (2^n - 1)^l, \quad i = 1, 2, \dots, 2^{n-1}. \quad (\text{B1})$$

$$\begin{cases} F_{(k-1) \cdot 2^{n-1+i}}^{C'} = g_k^{(l)} + f_i^{C'}, \\ F_{(k-1) \cdot 2^{n-1+i}}^{C''} = g_k^{(l)} + f_i^{C''}, \\ F_{(k-1) \cdot 2^{n-1+i}}^{D'} = g_k^{(l)} + f_i^{D'}, \\ F_{(k-1) \cdot 2^{n-1+i}}^{D''} = g_k^{(l)} + f_i^{D''}, \end{cases} \quad (\text{B2})$$

where

$$\begin{cases} f_{(i-1) \cdot 2^{n-m+k}}^{C'} = f_k^{B_2} + f_i^A, \\ f_{(i-1) \cdot 2^{n-m+k}}^{C''} = f_k^{B_1} + f_i^A, \quad i = 1, 2, \dots, 2^{m-1}, \\ f_{(i-1) \cdot 2^{n-m+k}}^{D'} = f_k^{B_2} - f_i^A, \quad k = 1, 2, \dots, 2^{n-m}, \\ f_{(i-1) \cdot 2^{n-m+k}}^{D''} = f_k^{B_1} - f_i^A. \end{cases} \quad (\text{B3})$$

The functions $r_k^{(l)}$, r_i^p , $g_k^{(l)}$, $f_k^{B_1}$, $f_k^{B_2}$, and f_i^A are the same as that expressed in (A1)–(A4) of Appendix A.

*Corresponding author. Tel.: +886-2-23659996; fax: +886-2-23631755. Email address: ccma@ntu.edu.tw

¹T. C. T. Ting, *Anisotropic Elasticity* (Oxford University Press, New York, 1996).

²S. G. Lekhnitskii, *Theory of Elasticity of an Anisotropic Body* (Holden-Day, San Francisco, CA, 1963).

³A. N. Stroh, *Philos. Mag.* **7**, 625 (1958).

⁴C. C. Ma, *AIAA J.* **34**, 2453 (1996).

⁵C. O. Horgan and K. L. Miller, *J. Appl. Mech.* **61**, 23 (1994).

⁶W. Yang and C. C. Ma, *Proc. R. Soc. London, Ser. A* **454**, 1843 (1998).

⁷A. K. Head, *Philos. Mag.* **44**, 92 (1953).

⁸T. C. T. Ting and D. M. Barnett, *Int. J. Solids Struct.* **30**, 92 (1993).

⁹J. Dundurs and G. P. Sandeckyj, *J. Appl. Phys.* **36**, 3353 (1965).

¹⁰D. M. Barnett and J. Lothe, *J. Phys. F: Met. Phys.* **4**, 1618 (1974).

¹¹Z. Suo, *Proc. R. Soc. London, Ser. A* **427**, 331 (1990).

¹²T. C. T. Ting, *Q. J. Mech. Appl. Math.* **45**, 119 (1992).

¹³D. M. Barnett and J. Lothe, *Int. J. Solids Struct.* **32**, 291 (1995).

¹⁴F. R. N. Nabarro and E. J. Kostlan, *J. Appl. Phys.* **49**, 5445 (1978).

¹⁵W. C. Moss and W. G. Hoover, *J. Appl. Phys.* **49**, 5449 (1978).

¹⁶Y. T. Chou, *J. Appl. Phys.* **34**, 3608 (1963).

¹⁷L. Stagni and R. Lizzio, *Int. J. Eng. Sci.* **4**, 471 (1986).

¹⁸K. C. Wu and Y. T. Chiu, *Int. J. Solids Struct.* **32**, 543 (1995).

¹⁹Y. T. Chiu and K. C. Wu, *J. Appl. Mech.* **44**, 424 (1998).

²⁰R. Weeks, J. Dundurs, and M. Stippes, *Int. J. Eng. Sci.* **6**, 365 (1968).

²¹M. S. Lee and J. Dundurs, *Int. J. Eng. Sci.* **11**, 87 (1973).

²²S. N. G. Chu, *J. Appl. Phys.* **53**, 3019 (1982).

²³Y. T. Chou, *Phys. Status Solidi* **17**, 509 (1966).

²⁴S. V. Kamat, J. P. Hirth, and B. Carnahan, *Scr. Metall.* **21**, 1587 (1987).

²⁵M. L. Öveçoğlu, M. F. Doerner, and W. D. Nix, *Acta Metall.* **35**, 2947 (1987).

²⁶R. L. Lin and C. C. Ma, *J. Appl. Mech.* **67**, 597 (2000).